

# RSC Advances



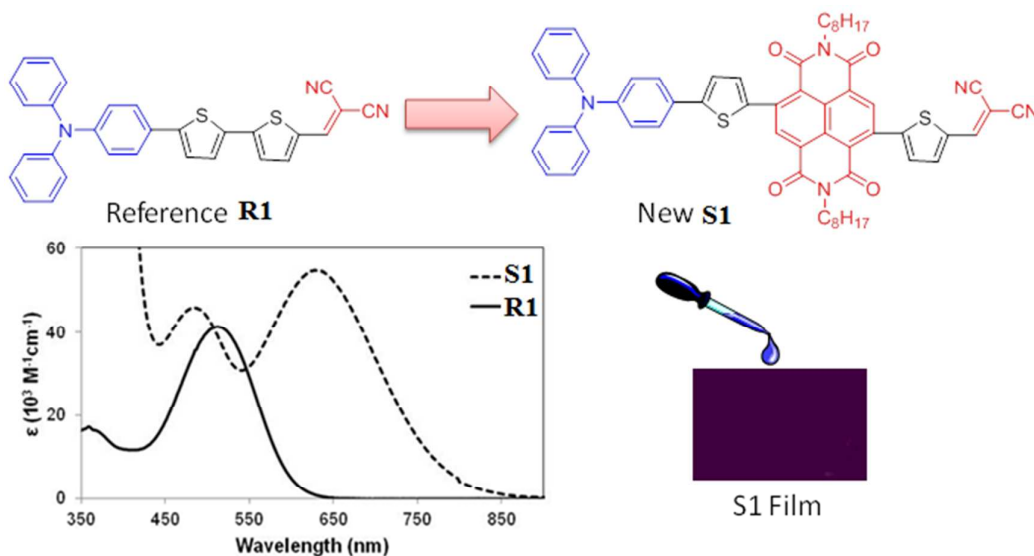
This is an *Accepted Manuscript*, which has been through the Royal Society of Chemistry peer review process and has been accepted for publication.

*Accepted Manuscripts* are published online shortly after acceptance, before technical editing, formatting and proof reading. Using this free service, authors can make their results available to the community, in citable form, before we publish the edited article. This *Accepted Manuscript* will be replaced by the edited, formatted and paginated article as soon as this is available.

You can find more information about *Accepted Manuscripts* in the [Information for Authors](#).

Please note that technical editing may introduce minor changes to the text and/or graphics, which may alter content. The journal's standard [Terms & Conditions](#) and the [Ethical guidelines](#) still apply. In no event shall the Royal Society of Chemistry be held responsible for any errors or omissions in this *Accepted Manuscript* or any consequences arising from the use of any information it contains.

## Graphical Abstract



Betterment of optoelectronic and photovoltaic properties is reported through the embodiment of a planar, conjugated naphthalene diimide functionality in a given donor-acceptor small molecular oligothiophene, when used in solution-processable bulk heterojunction solar cells.

## COMMUNICATION

# Improvement of optoelectronic and photovoltaic properties through the insertion of a naphthalenediimide unit in donor-acceptor oligothiophenes†

Cite this: DOI: 10.1039/x0xx00000x

Received 00th January 2012,  
Accepted 00th January 2012

DOI: 10.1039/x0xx00000x

www.rsc.org/

**Improvements to the optoelectronic and photovoltaic properties of 2-((5'-(4-(diphenylamino)phenyl)-[2,2'-bithiophen]-5-yl)methylene)malononitrile (R1; a donor-acceptor small molecular oligothiophene) are reported through the insertion of planar, conjugated naphthalenediimide moiety. The novel donor material was successfully synthesized and exhibited a power conversion efficiency of 3.01% under AM 1.5 G irradiation (100 mW cm<sup>-2</sup>) when tested in solution-processable bulk heterojunction solar cells with PC<sub>61</sub>BM as an acceptor material.**

In recent times, solution-processable bulk heterojunction (BHJ) solar cells have gained interest among many academic and industrial research groups as they have the potential to be lightweight, flexible and cost effective alternatives to the traditional solar-cells, besides, possess capability for simple mass production.<sup>1</sup> In the past 5 years, significant improvements have been achieved in the development of BHJ solar cells through a combination of efforts including the design of more active materials, morphology control, and device fabrication processes.<sup>2</sup> Traditionally, semiconducting polymers such as poly(3-hexylthiophene) (P3HT) are used as electron donor materials and soluble fullerene derivatives such as [6,6]-phenyl-C<sub>61</sub>-butyric acid methyl ester (PC<sub>61</sub>BM) are used as electron acceptor materials.<sup>3</sup> Recent reports, however, have described improvements in BHJ device performance by using small molecules and this in turn has drawn attention away from the more established polymeric semiconductors like P3HT.<sup>4</sup> These small molecules possess an advantage of being able to be synthesised and purified as single molecular entities, thus removing the major bottlenecks of device variability that can arise from material inconsistencies.

As with polymeric structures, the design requirements of small organic semiconductors include broad absorption profile, high charge mobility, multiple reversible redox potentials and appropriate energy difference in the highest occupied molecular orbital (HOMO) and lowest unoccupied molecular orbital (LUMO) energy levels. It has been established that low band gap materials can be generated by incorporating an electron donor- $\pi$ -bridge-acceptor (D- $\pi$ -A or D-A) motif within the structure.<sup>5,2a</sup> As previously discussed, reports of BHJ devices

using small organic molecules as donor components have recently emerged and have resulted in devices exhibiting power conversion efficiencies (PCEs) in excess of 9%.<sup>6</sup> Even though this progress is inspiring, ample scope still exists to develop novel light-harvesting materials that possess broad and efficient optical absorption, low HOMO energy levels (-5.0 to -5.5 eV) and adequate solubility required for solution processability.<sup>4</sup> One successful strategy to fulfil such requirements is the exploration of D-A based compounds that show charge transfer absorption. Key examples of this approach have been reported by various research groups.<sup>7</sup> Thus, there is considerable interest in exploring new D-A combinations and in synthesising molecules that can be processed from solution. In this communication, we report a strategy to investigate D-A design.

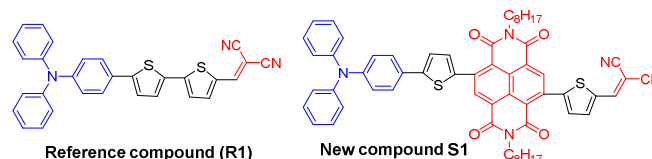


**Fig. 1** Molecular structures of the materials investigated in this work

We chose a triarylamine end-group as the donor component, a dicyanovinyl acceptor group and introduced a planar, conjugated naphthalenediimide (NDI) functionality in order to vary (1) the optoelectronic and photovoltaic properties, and (2) the processability of small organic molecules (Fig. 1). The NDI unit has interesting physical and electronic properties, and chromophores based on the NDI framework have been used as active components for organic electronic applications.<sup>8,4e</sup> An additional advantage of the NDI functionality is that a variety of alkyl groups can be located on the nitrogen atoms, thus allowing tuning of solubility. In the present case, the -octyl group was the substituent of choice for producing highly soluble compound with excellent film forming properties without crystallization occurring in the film, see compound 2-((5-(9-(5-(4-(diphenylamino)phenyl) thiophen-2-yl)-2,7-dioctyl-1,3,6,8-tetraoxo-1,2,3,6,7,8-hexahydro-benzo[*lmn*][3,8]phenanthroline-4-yl)thiophen-2-yl)methylene)malono nitrile (S1); Fig. 1. Newly designed S1 is deemed to exhibit enhanced solubility and a large red

shift of lambda maximum when compared with the reference compound **R1**. It is worth mentioning that compound **S1** is the first reported example where NDI unit has been incorporated in the D–A module for BHJ applications.

Compound **S1** was synthesized in moderate to high yields by reacting 5-(9-(5-(4-(diphenylamino)phenyl)thiophen-2-yl)-2,7-dioctyl-1,3,6,8-tetraoxo-1,2,3,6,7,8-hexahydrobenzo[*lmm*][3,8]phenanthroline-4-yl)thiophene-2-carbaldehyde with malononitrile, in acetonitrile:chloroform (1:1) solvent mixture at reflux with piperidine as a base (for detailed synthetic procedures, please see the electronic supplementary information (ESI<sup>†</sup>)). **S1** was purified by conventional column chromatography and was fully characterized by means of high resolution mass spectrometry and NMR spectroscopy. High solubility of small molecular semiconductors is an essential feature for the fabrication of solution-processable BHJ devices and **S1** meets this criterion as it displays high solubility in many routine solvents, such as chloroform (CHCl<sub>3</sub>), chlorobenzene and toluene (for instance, 25 mg/mL in CHCl<sub>3</sub>). Thermogravimetric analysis (TGA) revealed that **S1** exhibits excellent thermal stability (>250 °C), a finding that strongly supports the fact that the compound will remain active and stable during the high temperature annealing of organic photovoltaic devices (Fig. S1, ESI<sup>†</sup>). Reference compound **R1** was synthesized in our labs following the literature procedure.<sup>7e</sup>

The comparative UV–vis absorption spectral study of **S1** and **R1** was carried out in CHCl<sub>3</sub> solution (Fig. 2). The use of NDI functionality induces a strong red-shift in the absorption of compound **S1** when compared with **R1**. Typically, **S1** gives strong absorption band maximum ( $\lambda_{\text{max}}$ ) at 632 nm ( $\epsilon = 54,820 \text{ M}^{-1} \text{ cm}^{-1}$ ), and **R1** gives  $\lambda_{\text{max}}$  at 514 nm ( $\epsilon = 41,250 \text{ M}^{-1} \text{ cm}^{-1}$ ). With the use of NDI functionality we found >30% enhancement to the peak molar absorptivity of **S1** compared with **R1**. A note of interest is the fact that we observed the same bathochromic absorption shift in thin film spectrum of **S1** compared with that of **R1** (Fig. 2).

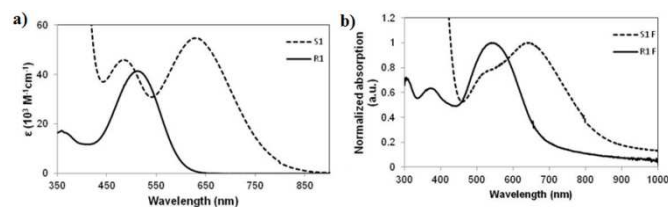


**Fig. 2** Absorption spectra of compounds **S1** and **R1** (a) in CHCl<sub>3</sub> solutions and (b) for pristine as-cast films (films of **S1** and **R1** were spin-cast at 3000 rpm for 1 min to give a film thickness of ~55 nm).

The absorption profile of **S1** in pristine state can be described as panchromatic with its absorption extending through the entire visible spectrum and tailing into the near infra-red region (400–1000 nm). This type of control in altering the absorption profile by incorporating a more strongly electron accepting moiety could lead to enhanced light harvesting properties in small molecular semiconductors.

Density functional theory (DFT) calculations using the Gaussian 09 suite of programs<sup>9</sup> and B3LYP/6-311+G(d,p)//B3LYP/6-31G(d) level of theory indicated that the HOMO orbital density of **S1** has a major distribution over triphenylamine donor functionality and the

LUMO density was delocalized through both acceptor functionalities, NDI and malononitrile, with almost equal contribution (Fig. 3). Such a segregation of HOMO and LUMO densities is an ideal condition for the intramolecular charge transfer (ICT) transition and is attributed to the presence of a strong acceptor unit, of which NDI is an example, in the given D–A system.

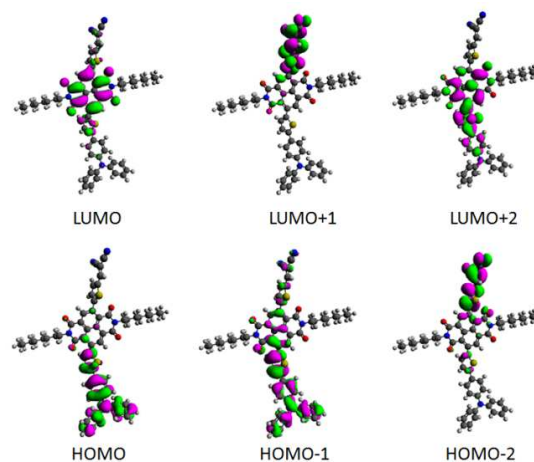


**Fig. 3** Orbital density distribution for the HOMOs (lower) and LUMOs (upper) of **S1**. DFT calculations were performed using the Gaussian 09 suite of programs and B3LYP/6-311+G(d,p)//B3LYP/6-31G(d) level of theory.

Experimental estimation of HOMO energies was carried out using photo electron spectroscopy in air (PESA) and the LUMO energies were calculated by adding the bandgap to the HOMO values (see Fig. 4 for energy level diagram, and Fig. S2 for PESA curve).

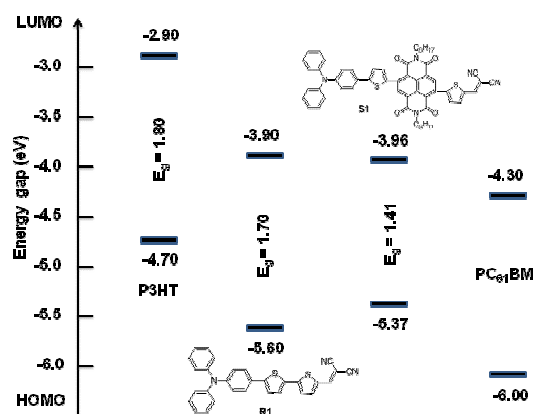


**Fig. 4** Energy level diagram depicting the band gaps of **S1** and **R1** in comparison with P3HT and PC<sub>61</sub>BM.

The UV–vis spectra indicated that insertion of NDI unit reduces the band gap of **S1** when compared with **R1**. PESA and UV–vis spectra indicated that the band gaps of these materials are all in the range required of donor materials for BHJ devices and are significantly narrower in magnitude than 1.8 eV measured for P3HT. The LUMO of **S1** was the lowest of two due to the bathochromic shift observed in the thin film spectrum when compared with **R1**. The optical and electrochemical properties of both the materials are summarized in Table S1 (see ESI<sup>†</sup>).

Initial screening into the potency of **S1** as a donor material (*p*-type) was carried out by using it in a solution-processed BHJ device with conventional *n*-type soluble fullerene derivative PC<sub>61</sub>BM, and its performance under simulated sunlight and monochromatic light illumination was characterized. BHJ architectures typically deliver higher power conversion efficiencies (PCEs) by maximising the surface area of interface between the *p*- and *n*-type materials in the active layer. The blend solution of **S1** and PC<sub>61</sub>BM was used to cast an active layer on top of the PEDOT:PSS surface. The BHJ device architecture used was ITO/PEDOT:PSS (38 nm)/active layer/Ca (20 nm)/Al (100 nm) where the active layer was a solution processed blend of **S1** and PC<sub>61</sub>BM. For **S1**, a promising PCE of 3.01% was achieved when the film was spin-coated from a chlorobenzene solution as a 1:1 blend with PC<sub>61</sub>BM. By contrast, the maximum PCE obtained for a device based on **R1** was 1.10%, when fabricated under similar conditions. The comparative current–voltage curves for the optimized blends of **S1** and **R1** with PC<sub>61</sub>BM are shown in Fig. 5.

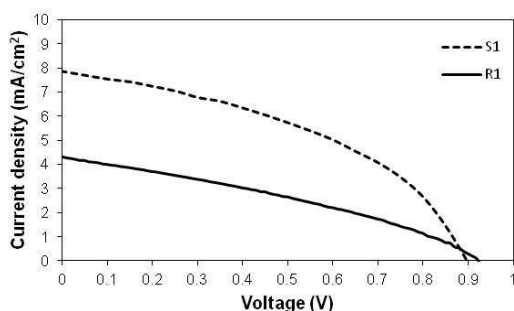


**Fig. 5** Current–voltage curves for the optimized devices based on **S1** and **R1** in blends with PC<sub>61</sub>BM (1:1 wt.) under simulated sunlight (AM 1.5, 1000 W/m<sup>2</sup>). Device Structure is: ITO/PEDOT:PSS (38 nm)/Active layer/Ca (20 nm)/Al (100 nm) where the active layers were the blends of materials and PC<sub>61</sub>BM spun on top of the films of PEDOT:PSS using chlorobenzene.

The optimized devices based on **S1** showed lower open circuit voltages ( $V_{oc}$ ) than the devices based on **R1**. These values are consistent with the measured HOMO values where the more positive HOMO for compound **S1** would predict a lower  $V_{oc}$ . Devices based on **S1** showed higher photocurrent than the devices based on **R1**, a finding that is consistent with the observed bathochromic-shift in the absorption spectrum of **S1** compared with **R1**. The BHJ devices based on **S1** yielded promising performance and the photovoltaic cell parameters,  $V_{oc}$ , short circuit current density ( $J_{sc}$ ), fill factor (FF) and PCE, reached 0.90 V, 7.90 mA/cm<sup>2</sup>, 0.43 and 3.01%, respectively. Overall, the insertion of NDI functionality into the studied D–A module resulted in around 80% increase in the photocurrent density and enhanced the PCE by a factor of >2, thus promoting the use of an electron accepting and highly conjugated functionality as an interesting structural concept for the design and development of highly efficient BHJ materials. With regards to the processing conditions of blend solutions, it has been shown<sup>4a</sup> that there exists a strong relationship between the degree of crystallization and solvent selection on the cell performance. Our attempts to fabricate devices using low boiling solvents, such as CHCl<sub>3</sub>, resulted in very poor photovoltaic performance. This was

primarily due to low film quality. The use of high-boiling solvent is further preferable from a processing point of view.

The incident-photon-to-current conversion efficiency (IPCE) curves of the best BHJ devices based on these small molecules under monochromatic light are shown in Fig. 6. The analysis of the IPCE measurements of these BHJ devices reveals a significantly higher and broader peak IPCE of **S1** (~42% @ 640 nm) compared to **R1** (38% @ 515 nm), which is presumably caused by the synergistic effect of excellent light-harvesting and tuned electrochemical properties. The IPCE measurements reported here are comparable to the film absorptions of **S1** and **R1** which indicate that the current arises mainly from the *p*-type donor material. Note that **S1** shows light harvesting and electrochemical properties that are largely superior to **R1**, which translates to higher conversion efficiency.

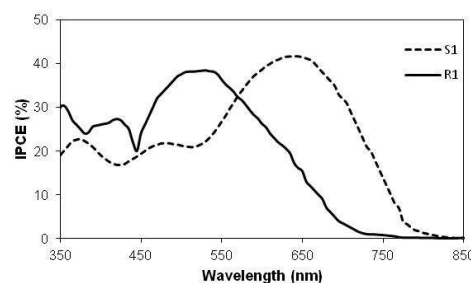


**Fig. 6** Comparative IPCE curves of the best BHJ devices based on **S1** and **R1**.

The active layer morphology was examined by an atomic force microscope (AFM) technique in tapping mode. The actual surface morphology of blend film of **S1**:PC<sub>61</sub>BM (1:1, w/w; as cast) is depicted in Fig. 7. The as casted film exhibited crystalline grains with a root-mean-square (RMS) roughness of 0.32 nm. The crystalline grains may be beneficial to ordered structure formation and charge transport in thin film. The hole only mobility in the BHJ blend film was measured by a space-charge limited current (SCLC) method with device structure of ITO/PEDOT:PSS/Active layer/Au. A hole mobility of  $8.5 \times 10^{-6} \text{ cm}^2 \text{ V}^{-1} \text{ s}^{-1}$  was obtained for the blend of **S1** and PC<sub>61</sub>BM.

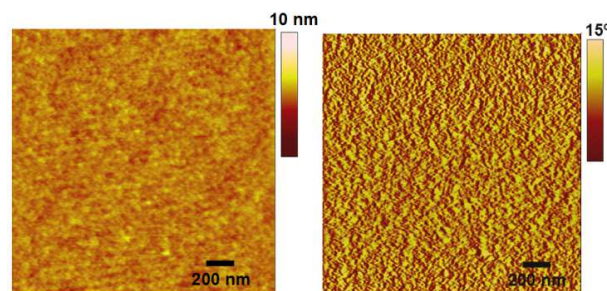


**Fig. 7** AFM image of 1:1 blend film with PC<sub>61</sub>BM spin-casted from chlorobenzene at 2500 rpm atop annealed ITO/PEDOT:PSS substrate. Topographic image (as-cast) with RMS 0.32 nm of **S1**:PC<sub>61</sub>BM.

Even though the progress in the development of small molecular donors is on surge, the material reported in this paper has highlighted the potential for efficiency improvements in a given D–A system. The discovery of such materials exhibiting promising optoelectronic properties opens up a way to develop such motifs (based on the

insertion of highly conjugated, planar functionality) and paves the way for such materials to be used for other organic electronic applications such as organic field-effective transistors.

In conclusion, we have demonstrated the first use of a NDI functionality to improve the optoelectronic and photovoltaic properties of D–A small molecules in organic solar cells. In a direct comparison we have shown that the incorporation of this electron accepting, highly conjugated and planar system lowers the band gap of an oligothiophene dye, **S1**, and shows higher PCE compared with an analogue, **R1**. **S1** showed excellent thermal stability and solubility in common organic solvents, strong optical absorption over the whole visible region, low lying HOMO energy level and good photovoltaic performance. Based on the optoelectronic characterization and BHJ parameters, it is evident that the design concept addressed herein has huge potential to generate a series of novel organic materials whose properties can be tailored towards their use in conjunction with alternative accepting functionalities. We strongly believe that **S1** represents a valuable addition to the library of small molecular electron donors that will form the basis for next generation of custom-designed high-efficiency materials.

### Acknowledgements

Sid. V. B. would like to thank the TAPSUN programme for financial assistance under the project NWP0054 and V. Jayathirtha Rao for providing facilities. S. R. B. would like to thank CSIR, New Delhi for SRF fellowship. Sh. V. B. acknowledges Australian Research Council for financial support through a Future Fellowship Scheme (FT110100152). A. G. acknowledges CSIRO and the RMIT University for a visiting fellow position. A. G. acknowledges the assistance of Dr Jegadesan Subbiah (Bio21 Institute, University of Melbourne) for providing support during the fabrication of BHJ devices.

### Notes and references

<sup>a</sup> Polymers and Functional Materials Division, CSIR-Indian Institute of Chemical Technology, Hyderabad 500007, Telangana, India;

[bhosale@iict.res.in](mailto:bhosale@iict.res.in)

<sup>b</sup> Medicinal Chemistry, Monash Institute of Pharmaceutical Sciences, Monash University, Parkville VIC 3052, Australia;

[akhil.gupta@monash.edu](mailto:akhil.gupta@monash.edu)

<sup>c</sup> School of Applied Sciences, RMIT University, GPO Box 2476, Melbourne VIC 3001, Australia; E-mail: [sheshanath.bhosale@rmit.edu.au](mailto:sheshanath.bhosale@rmit.edu.au)

<sup>d</sup> CSIRO Manufacturing, Virtual Nanoscience Lab, Parkville Victoria 3052, Australia

<sup>1</sup> SRB and AG contributed equally to this work.

† Electronic Supplementary Information (ESI) available: [Synthetic procedures, **S1** spectra, PESA and TGA curves]. See

DOI: 10.1039/c000000x/

- (a) G. Yu, J. Gao, J. C. Hummelen, F. Wudl and A. J. Heeger, *Science*, 1995, **270**, 1789; (b) G. Li, V. Shrotriya, J. S. Huang, Y. Yao, T. Moriarty, K. Emery and Y. Yang, *Nat. Mater.*, 2005, **4**, 864; (c) S. H. Park, A. Roy, S. Beaupre, S. Cho, N. Coates, J. S. Moon, D. Moses, M. Leclerc, K. Lee and A. J. Heeger, *Nat. Photonics*, 2009, **3**, 297; (d) Y. Liang, Z. Xu, J. Xia, S.-T. Tsai, Y. Wu, G. Li, C. Ray and L. Yu, *Adv. Mater.*, 2010, **22**, E135; (e) S. B. Darling and F. You, *RSC Adv.*, 2013, **3**, 17633.
- (a) S. Günes, H. Neugebauer and N. S. Sariciftci, *Chem. Rev.*, 2007, **107**, 1324; (b) B. C. Thompson and J. M. J. Frechet, *Angew. Chem. Int. Ed.*, 2008, **47**, 58; (c) X. Yang and J. Loos, *Macromolecules*, 2007, **40**, 1353; (d) B. Kippelen and J.-L. Brédas, *Energy Environ. Sci.*, 2009, **2**, 251; (e) Y.-J. Cheng, S.-H. Yang and C.-S. Hsu, *Chem. Rev.*, 2009, **109**, 5868.
- (a) A. Facchetti, *Chem. Mater.*, 2011, **23**, 733; (b) H. Patil, W. X. Zu, A. Gupta, V. Chellappan, A. Bilic, P. Sonar, A. Rananaware, S. V. Bhosale and S. V. Bhosale, *Phys. Chem. Chem. Phys.*, 2014, **16**, 23837; (c) A. Gupta, S. E. Watkins, A. D. Scully, Th. B. Singh, G. J. Wilson, L. J. Rozanski, and R. A. Evans, *Synth. Met.*, 2011, **161**, 856; (d) A. M. Raynor, A. Gupta, H. Patil, A. Bilic and S. V. Bhosale, *RSC Adv.*, 2014, **4**, 57635.
- (a) B. Walker, C. Kim and T.-Q. Nguyen, *Chem. Mater.*, 2011, **23**, 470; (b) Y. Li; Q. Guo, Z. Li, J. Pei and W. Tian, *Energy Environ. Sci.*, 2010, **3**, 1427; (c) J. E. Anthony, *Chem. Mater.*, 2011, **23**, 583; (d) A. Mishra and P. Bäuerle, *Angew. Chem. Int. Ed.*, 2012, **51**, 2020; (e) Y. Lin, Y. Li and X. Zhan, *Chem. Soc. Rev.*, 2012, **41**, 4245.
- (a) B. C. Thompson and J. M. Fréchet, *Angew. Chem. Int. Ed.*, 2008, **47**, 58; (b) G. Dennler, M. C. Scharber and C. J. Brabec, *Adv. Mater.*, 2009, **21**, 1323; (c) J. Chen and Y. Cao, *Acc. Chem. Res.*, 2009, **42**, 1709; (d) Y.-J. Cheng, S.-H. Yang and C. -S. Hsu, *Chem. Rev.*, 2009, **109**, 5868; (e) Y. Li and Y. Zou, *Adv. Mater.*, 2008, **20**, 2952.
- (a) Z. Li, G. He, X. Wan, Y. Liu, J. Zhou, G. Long, Y. Zuo, M. Zhang and Y. Chen, *Adv. Energy Mater.*, 2012, **2**, 74; (b) T. S. Vander Poll, J. A. Love, T.-Q. Nguyen, G. C. Bazan, *Adv. Mater.*, 2012, **24**, 3646; (c) J. Zhou, X. Wan, Y. Liu, Y. Zuo, Z. Li, G. He, G. Long, W. Ni, C. Li, X. Su and Y. Chen, *J. Am. Chem. Soc.*, 2012, **134**, 16345; (d) V. Gupta, A. K. K. Kyaw, D. H. Wang, S. Chand, G. C. Bazan and A. J. Heeger, *Sci. Rep.*, 2013, **3**, 1965; (e) J. Zhou, Y. Zuo, X. Wan, G. Long, Q. Zhang, W. Ni, Y. Liu, Z. Li, G. He, C. Li, B. Kan, M. Li and Y. Chen, *J. Am. Chem. Soc.*, 2013, **135**, 8484.
- (a) N. M. Kronenberg, M. Deppisch, F. Würthner, H. W. A. Lademann, K. Deing and K. Meerholz, *Chem. Commun.*, 2008, 6489; (b) N. M. Kronenberg, V. Steinmann, H. Bürckstümmer, J. Hwang, D. Hertel, F. Würthner and K. Meerholz, *Adv. Mater.*, 2010, **22**, 4193; (c) A. B. Tamayo, X.-D. Dang, B. Walker, J. Seo, T. Kent and T.-Q. Nguyen, *Appl. Phys. Lett.*, 2009, **94**, 103301; (d) B. Walker, A. B. Tamayo, X.-D. Dang, P. Zalar, J. H. Seo, A. Garcia, M. Tantiwiwat and T.-Q. Nguyen, *Adv. Funct. Mater.*, 2009, **19**, 1; (e) A. Gupta, A. Ali, A. Bilic, M. Gao, K. Hegedus, B. Singh, S. E. Watkins, G. J. Wilson, U. Bach and R. A. Evans, *Chem. Commun.*, 2012, **48**, 1889; (f) A. Gupta, V. Armel, W. Xiang, G. Fanchini, S. E. Watkins, D. R. MacFarlane, U. Bach and R. A. Evans, *Tetrahedron*, 2013, **69**, 3584; (g) R. J. Kumar, Q. I. Churches, J. Subbiah, A. Gupta, A. Ali, R. A. Evans and A. B. Holmes, *Chem. Commun.*, 2013, **49**, 6552; (h) A. Gupta, A. Ali, Th. B. Singh, A. Bilic, U. Bach and R. A. Evans, *Tetrahedron*, 2012, **68**, 9440; (i) A. Gupta, A. Ali, A. Bilic, Th. B. Singh and R. A. Evans, *Dyes Pigments*, 2014, **108**, 15.
- (a) S. V. Bhosale, C. Jani and S. Langford, *Chem. Soc. Rev.*, 2008, **37**, 331; (b) H. Patil, A. Gupta, A. Bilic, S. V. Bhosale and S. V. Bhosale, *Tetrahedron Lett.*, 2014, **55**, 4430; (c) H. Patil, A. Gupta, A. Bilic, S. L. Jackson, K. Latham and S. V. Bhosale, *J. Electron. Mater.*, 2014, **43**, 3243.
- M. J. Frisch, *et al.*, Gaussian 09 revision D.01, Gaussian Inc. Wallingford CT, 2013.